



International Journal of Information and Communication Technology

ISSN online: 1741-8070 - ISSN print: 1466-6642
<https://www.inderscience.com/ijict>

Research on high-precision time synchronisation technology for sea mobile platforms

Dao Peng Dong, Hong Shuo Wu, Qing Feng Guo, Jin Wei Yang, Xi Li

DOI: [10.1504/IJICT.2024.10063506](https://doi.org/10.1504/IJICT.2024.10063506)

Article History:

Received:	17 January 2024
Last revised:	19 February 2024
Accepted:	24 February 2024
Published online:	12 May 2024

Research on high-precision time synchronisation technology for sea mobile platforms

Dao Peng Dong*

Cheng Du Spaceon Electronics Co., Ltd.,
Cheng Du 610036, China

and

Laboratory of Science and Technology on Marine
Navigation and Control,
China State Shipbuilding Corporation,
300131, China

Email: 417485594@qq.com

*Corresponding author

Hong Shuo Wu

Tianjin Institute of Navigation Instruments,
300131, China

Email: whszi1988@163.com

Qing Feng Guo, Jin Wei Yang and Xi Li

Cheng Du Spaceon Electronics Co., Ltd.,
Cheng Du 610036, China

Email: gqf19861019@163.com

Email: 446154505@qq.com

Email: 779617448@qq.com

Abstract: Under static conditions, at present, mature technologies for long-distance and high-precision time synchronisation include satellite common view (CV) and two-way satellite time and frequency transfer (TWSTFT) and so on. However, under dynamic conditions, research on high-precision time synchronisation technology is relatively lacking such as mobile platforms on the sea. Considering the dynamic conditions of mobile platforms on the sea, a method of position's smooth filtering with velocity is proposed to improve the accuracy of position measurement, reducing the time measurement error introduced by position error. The proposed method ultimately improves the CV comparison accuracy between sea surface mobile platforms. The simulation and actual test results show that by using the method of position's smooth filtering with velocity, the CV comparison accuracy between mobile platforms on the sea can reach 10 ns.

Keywords: mobile platform; time and frequency synchronisation; spaceon electronics; common view; CV.

Reference to this paper should be made as follows: Dong, D.P., Wu, H.S., Guo, Q.F., Yang, J.W. and Li, X. (2024) ‘Research on high-precision time synchronisation technology for sea mobile platforms’, *Int. J. Information and Communication Technology*, Vol. 24, No. 6, pp.57–70.

Biographical notes: Dao Peng Dong received his PhD in Astrometry and Astromechanics from University of Chinese Academy of Sciences, Beijing, China in 2015. He engaged in research on precision time-frequency measurement technology. From 2008 to 2018, he worked in National Time Service Center (NTSC). From 2019 to 2023, he worked in Cheng Du Spaceon Electronics Co., Ltd. He has obtained a Senior Engineer.

Hong Shuo Wu received his MS in Control Science and Engineering from Tianjin University, TianJin, China in 2014. He engaged in research on precision time-frequency measurement technology. From 2014 to 2023, he worked in Tianjin Institute of Navigation Instruments. He has obtained a Senior Engineer.

Qing Feng Guo received his MS in Control Science and Engineering from Southwest Jiaotong University, Chengdu, China in 2013. He engaged in research on precision time-frequency transmit technology by GNSS. From 2014 to 2023, he worked in Cheng Du Spaceon Electronics Co., Ltd.

Jin Wei Yang received his BS in Electronic and Communication Engineering from Shenyang Ligong University. He engaged in research on precision time-frequency measurement technology. From 2018 to 2023, he worked in Cheng Du Spaceon Electronics Co., Ltd.

Xi Li received her MS in Electronic and Communication Engineering from University of Electronic Science and Technology, Chengdu, China in 2021. She engaged in research on precision time-frequency measurement technology by GNSS. From 2021 to 2023, she worked in Cheng Du Spaceon Electronics Co., Ltd.

1 Introduction

With the rapid development of information technology, the traditional work mode has undergone fundamental changes, which changes from the original platform independent working mode to the network centre collaborative working mode. The CEC (collaborative work capability) system of the US aircraft carrier fleet is a model of collaborative defence work in the new era. This system combines independent work units by fully utilising information systems such as computers, data links, and navigation to form organic work entities, supporting unified work actions. Collaborative work is an inevitable trend for future development. To achieve collaborative work, it is necessary to achieve a high degree of unity in the spatiotemporal benchmark of the workspace, and the collaborative work of information weapons and equipment heavily relies on spatiotemporal unity.

An accurate coordinate system and time system are the basic prerequisites for ship command, testing, and drills. The shipborne time system provides unified and accurate time information, time marking information, or agreed time control signals for the equipment in the ship. The characteristics of ship formation command, testing, and drills

determine the wide distribution of command units, and each ship needs to cooperate with each other to complete common tasks. To coordinate the work of all ship mounted equipment and obtain accurate and reliable data and information, it is necessary to achieve unified time and frequency across the entire system.

At present, research for time synchronisation technology mainly focuses on time synchronisation between devices or stations under static conditions. With the increasing popularity of cluster or formation collaborative application modes, it is increasingly important to study high-precision time synchronisation technology under dynamic conditions. In this paper, considering sea surface mobile platforms, a method is studied for improving the CV comparison accuracy under dynamic conditions, in which theoretical evaluation and practical experiments are used.

2 Basic principles of satellite CV synchronisation technology

Global satellite navigation system common view time comparison (GNSS CV) is one of the high-precision remote time transfer technologies used in time synchronisation technology. It has the characteristics of high comparison accuracy, wide coverage, low usage cost, and sustainable operation. CV time synchronisation refers to the simultaneous observation of the same visible satellite by two stations located at different positions. With a short baseline, satellite orbit, clock bias, ionospheric delay error, and tropospheric delay error can all be effectively eliminated. Before providing precise orbit and precise clock deviation, a timing accuracy of 3-5 ns can be achieved.

In an ideal condition, it is assumed that the Beidou or GPS receiver is placed at two known positions A and B respectively, which observes the same satellite i at the same time (Yang et al., 2021; Lu et al., 2020). Therefore:

Clock difference between clock A and satellite i :

$$\Delta t_{iA} = (t_i - t_A) \quad (1)$$

Clock difference between clock B and satellite i :

$$\Delta t_{iB} = (t_i - t_B) \quad (2)$$

The clock difference between station A and station B can be obtained by difference between above two equations:

$$\Delta t_{iA} - \Delta t_{iB} = (t_i - t_A) - (t_i - t_B) = t_B - t_A = t_{AB} \quad (3)$$

In practical applications, the CV principle is shown in Figure 1, considering the path delay of Beidou or GPS signals during transmission.

It is assumed that the clock time at station A is t_A , the clock time at station B is t_B , the GPS time is t_{GPS} , and d_A and d_B are path delays from the satellite to station A and station B respectively. The principle of accurate time difference measurement between station A and station B is as follows:

The CV receivers receive the same satellite signal at the same time, and send the second pulse, which represents BD/GPS time output by the receiver, to the high-precision time interval measurement module. And the second pulse output by the receiver is compared to the second pulse output by the local clock to obtain the time differences

between the receivers and the same satellite, which are represented by Δt_{AGPS} and Δt_{BGPS} respectively. In detail, equations are as follows:

$$\Delta t_{AGPS} = t_A - (t_{GPS} + d_A) \quad (4)$$

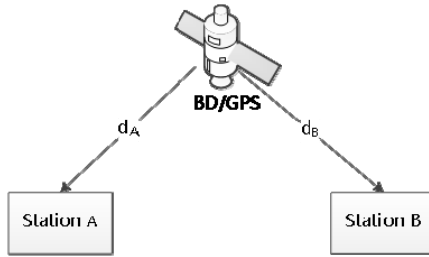
$$\Delta t_{BGPS} = t_B - (t_{GPS} + d_B) \quad (5)$$

The data from A and B is transferred to each other's computer through the communication network, where d_A and d_B can be calculated through satellite ephemeris. And the time difference between the two clocks can be obtained by difference between the above two equations, which is shown in the following equation:

$$\begin{aligned} \Delta t_{AGPS} - \Delta t_{BGPS} &= t_A - t_{GPS} - d_A - (t_B - t_{GPS} - d_B) \\ &= (t_A - t_B) - (d_A - d_B) \end{aligned} \quad (6)$$

It can be seen that CV can eliminate the influence of Beidou/GPS satellite clocks and most path additional delay, improving time synchronisation accuracy.

Figure 1 Schematic diagram of CV principle



3 An algorithm for reducing time difference measurement errors on sea surface mobile platforms

In high-precision time transfer under static conditions, the error introduced by position coordinates is minimised by antenna position's accurate measurement in advance or accumulating measurements over a long period of time. In dynamic environments, it is not possible to obtain accurate positions in real time, and the error introduced by antenna coordinates increases, which is the main error source of resulting in CV comparison accuracy attenuation under dynamic conditions. Therefore, improving position accuracy can significantly improve time transfer accuracy in dynamic environments (Yang et al., 2018).

The position accuracy can be improved by using position's smooth filtering with velocity. Due to the velocity is measured by carrier loop, whose accuracy is one order of magnitude higher than the position accuracy. Position accuracy can achieve 0.3m–1m by using position's smooth filtering with velocity. The detail filtering algorithm is as follows:

It is assumed that a scalar $\tilde{x}_1, \tilde{x}_2, \tilde{x}_3, \dots$ is one of the coordinate component of the user's position in a certain coordinate system which changes over time, such as the X

component in the WGS-84 geocentric Cartesian coordinate system or the latitude in the geodetic coordinate system. And the receiver's least squares positioning solution can also be considered as a position measurement. Due to the measurements or positioning solutions in scalar $\tilde{x}_1, \tilde{x}_2, \tilde{x}_3, \dots$ are generally rough, therefore, the filtered results are usually closer to the true position coordinates of the object.

It is assumed that \hat{x}_{k-1} and $\hat{\dot{x}}_{k-1}$ are filtering result after obtaining position measurement at $k-1^{\text{th}}$ instant, where \hat{x}_{k-1} is position estimation of user's true position x_{k-1} , and $\hat{\dot{x}}_{k-1}$ is the velocity estimation of user's true velocity \dot{x}_{k-1} . Therefore user's true position at k^{th} instant can be predicted by the velocity estimation $\hat{\dot{x}}_{k-1}$.

$$\hat{x}_k^- = \hat{x}_{k-1} + \hat{\dot{x}}_{k-1} T_s \quad (7)$$

where T_s represents the time interval between two adjacent measurement instants. The superscript '^' is used to represent estimation to distinguish it from the actual measurement represented by the superscript '~'. While the right superscript '-' in \hat{x}_k^- represents the prior estimation before obtaining and utilising the measurement \tilde{x}_k . It is assumed that the user's motion velocity remains constant or changes slightly during measurement interval, i.e. the velocity prior estimation is:

$$\hat{\dot{x}}_k^- = \hat{\dot{x}}_{k-1} \quad (8)$$

After obtaining the position measurement of the k epoch, the user's position estimation and velocity estimation are updated at the current time using the following two formulas:

$$\hat{x}_k = \hat{x}_k^- + \alpha (\tilde{x}_k - \hat{x}_k^-) \quad (9)$$

$$\hat{\dot{x}}_k = \hat{\dot{x}}_k^- + \frac{\beta}{T_s} (\tilde{x}_k - \hat{x}_k^-) \quad (10)$$

where α and β are two fixed filtering coefficients. It can be seen from the equations, α, β filter attempts to balance the position prior estimation with the latest measurement. And similar processes are used for the velocity. If α and β are larger, the weight on the current measurement value is higher. The necessary and sufficient condition for the stability of α, β filter is as follows:

$$0 < \alpha, 0 < \beta < 4 - 2\alpha \quad (11)$$

Generally, α and β are positive numbers less than 1.

The above equation can be expressed concisely in matrix form as follows:

$$\hat{x}_k^- = \begin{bmatrix} 1 & T_s \\ 0 & 1 \end{bmatrix} \hat{x}_{k-1} \quad (12)$$

$$\hat{x}_k = \hat{x}_k^- + \begin{bmatrix} \alpha \\ \beta / T_s \end{bmatrix} (\tilde{x}_k - [1 \ 0] \hat{x}_k^-) \quad (13)$$

where vector $\hat{x}_k^- = [\hat{x}_k^- \quad \hat{x}_k^-]^T$, vector $\hat{x}_k = [\hat{x}_k \quad \hat{x}_k]$.

In practical engineering applications by using proposed method, it is found that position accuracy can be improved to within 1m.

4 Evaluation of CV accuracy under sea surface mobile platforms

The main factors affecting the accuracy of co view comparison include geometric delay errors caused by satellite ephemeris, ionospheric delay correction model errors, tropospheric delay correction model errors, multipath errors introduced by receiver antennas, and the influence of system errors introduced by the equipment itself.

The ionospheric delay error correction technology using a dual frequency ionospheric correction model, the tropospheric delay error correction technology based on an improved Hopfield model, and the real-time calculation technology for precise position and clock deviation weaken the ionospheric and tropospheric delay errors and time difference measurement errors.

a *Errors introduced by dynamic environments*

The position accuracy can be improved within 1m in dynamic environments by using the method of position's smooth filtering with velocity. Therefore, the time error introduced by the position is approximately:

$$\sigma_{dyn} = 1 \times 3.3ns = 3.3ns$$

b *Geometric delay error introduced by satellite ephemeris*

The geometric delay is the distance delay between the navigation satellite and the ground receiver, therefore, geometric delay error is composed of the navigation satellite coordinate error and the receiver position error (Andreas et al., 2019; Guang et al., 2020; Tavella and Petit, 2020). The satellite position is calculated based on the satellite ephemeris, and the accuracy of satellite ephemeris broadcasted by the navigation satellite affects the accuracy of satellite position. During CV comparison, the satellite position error's impact on the geometric delay of two stations is unequal, making it impossible to completely offset geometric delay error. The remaining error can be estimated by the following equation

$$\sigma_{eph} = \frac{D'_{ab} \times d\bar{X}'_S}{c \times \rho} \quad (14)$$

where σ_{eph} is the clock difference error of two stations introduced by satellite ephemeris;

D'_{AB} Distance between two stations

$d\bar{X}'_S$ Satellite position error introduced by satellite ephemeris

ρ Distance between station and satellite.

The impact of receiver position on inter station time synchronisation accuracy mainly depends on the relative measurement accuracy of two stations. Considering the high position accuracy of the receiver, typically around 5 metres, error

introduced by radial component is relatively small, whose mean square error $\sigma_{rec} \leq 1\text{ns}$.

When the distance between two stations is 2,000 km, the clock difference error between two stations introduced by satellite ephemeris error is about 2.8 ns.

c *Ionospheric correction error*

The ionosphere is the atmosphere located between 50–1,000 km. Due to the sun's strong radiation, some gas molecules in the ionosphere will be ionised to form a large number of free electrons and positive ions (Panfilo et al., 2020; Zhang et al., 2018; Jiang et al., 2019). When electromagnetic wave signals pass through the ionosphere, the propagation path and velocity will change. Therefore, multiplying the signal propagation time by the propagation velocity in vacuum is not equal to the actual propagation distance of the signal, resulting in ranging errors, which are called ionospheric delay error. During CV comparison, if the distance between two stations is less than 1,000 km, the correlation between ionospheric parameters is large, which can offset most of the error. When the distance exceeds 1,000 km, the correlation between ionospheric parameters weakens. To reduce ionospheric correction error, a dual frequency correction model is used to correct the ionospheric delay, where pseudorange measurements at different frequencies are used. The dual frequency correction model for correcting ionospheric delay at B1 frequency using pseudorange measurements of B1 and B3 is as follows

$$\tau_{ion}(B_1) = \frac{1}{c} \frac{\rho_{B_3} - \rho_{B_1}}{a^2 - 1} \quad (15)$$

where ρ_{B_1} and ρ_{B_3} represent the pseudorange measurements at B1 and B3

respectively, and $a = \frac{f_1}{f_2}$ is the proportional constants of B1 and B3. For the Beidou

navigation system, the ionospheric delay is approximately 54.5ns. About 95% of the ionospheric delay can be eliminated by using a dual frequency correction model, which results in a remaining error of about 2.8ns. If distance between two stations is 2,000 km, the two paths from the satellite to two stations have a spatial correlation of 60%. After subtracting two paths, the ionospheric delay error is further reduced to 1.84ns, that is:

$$\sigma_{ion} = 1.84\text{ns}$$

d *Tropospheric correction error*

The troposphere is an atmosphere less than 40 km. When electromagnetic waves pass through the troposphere, propagation speed will change, causing propagation delay. Tropospheric correction error's magnitude is mainly related to pressure, temperature, humidity, and satellite elevation (Zhou et al., 2019; Geng et al., 2019). The 'Hopfield' model is used for calibration.

The path length difference introduced by tropospheric delay (i.e. the path length corresponding to the additional delay) is shown as follows:

$$\Delta S_{tro} = \int_{satellite}^{dev} (n-1)ds \quad (16)$$

The integral in the equation follows the signal path, where n is the refractive index. For the delay model of the troposphere, in the absence of real-time meteorological data, even in the cold weather of -20°C with a satellite altitude angle of about 45 degrees, the maximum errors caused by meteorological parameter temperature and atmospheric pressure errors are about 1.27ns and 1.23ns, and the maximum total error is 2.5ns. Considering that the two paths have 60% spatial correlation, the mean square error of the delay introduced into the process is 1.75ns, that is:

$$\sigma_{tro} = 1.75ns$$

e *Errors introduced by multipath effects*

Multipath is one of main error sources during receiver measurement. The generation of multipath is related to the site and surrounding environment of the antenna. Considering that the surrounding environment, elevation, and azimuth of two stations are all not same, the multipath impact is completely unrelated. The impact of multipath can be reduced by using anti-multipath interference antennas, selecting high-performance receivers, arranging antenna positions reasonably, and increasing the elevation angle of observation satellites. In this way, the introduced mean square error is 1.5ns through actual testing, that is:

$$\sigma_{multipath} = 1.5ns \quad (17)$$

f *The random error introduced by the device itself*

In addition to satellite ephemeris, ionosphere, troposphere, multipath effects, and errors introduced by the equipment itself, error introduced by the punctuality of CV interaction period, receiver measurement noise, and receiver delay calibration error are approximately:

$$\sigma_{syn} = 3.6ns \quad (18)$$

g *Time measurement error correction*

In time transmission, time measurement error refers to the error caused by the pseudo range observation accuracy of the user receiver. Since the pseudorange is measured by the method of capturing code signals, it is evident that the time measurement error depends on the code frequency (or symbol width) and the accuracy of receiver related processing. In order to weaken the impact of this error, narrow correlation technology and carrier smoothing method with code phase are adopted in this scheme.

- *Narrow correlation technology*: The correlator can improve the tracking accuracy of the code phase by setting a narrow correlation interval, while also reducing errors caused by multipath interference. The non-integer multiple sampling technique not only improves the accuracy of pseudocode tracking, but also does not require an increase in sampling rate or processing speed of digital devices, resulting in excellent cost-effectiveness for receivers using this technology.
- *Carrier smoothing of code phase*: Most receivers can smooth the code phase by fusing coarse code phase values and Doppler measurements, but the tracking accuracy of the code phase can be further improved through carrier phase values. According to the principle of carrier phase smoothing pseudorange, it is to smooth large-scale code pseudorange observations with small-scale phase observations to improve accuracy. The following formula is used:

$$\rho_{s,k} = \frac{1}{M} \rho_k + \frac{M-1}{M} [\rho_{s,k-1} + \lambda(\phi_k - \phi_{k-1})]$$

M Receiver count value

$\rho_{s,k}$ Pseudorange measured by receiver

ϕ Carrier phase.

h Receiver channel delay consistency error

A programmable logic circuits (FPGA) as the main hardware platform is used in the signal processing module. Internally, it contains multiple completely independent signal processing channels to complete algorithms such as pseudocode capture, tracking, and demodulation. Due to being multiple independent processing channels, there is theoretically inconsistency in signal processing delay. By taking the following measures, inconsistency in latency across different channels has been avoided:

Using global reset signal: Each signal processing channel adopts a unified global reset signal to ensure that each channel starts working simultaneously based on the same time reference point.

Using global clock and PLL phase-locked loop: The FPGA uses a global high-frequency clock internally. When laying out and wiring the FPGA, priority is given to wiring the global high-frequency clock to ensure zero clock delay to each FPGA module. And in the processing that requires synchronisation, a synchronous clock enable scheme is adopted, all using synchronous timing circuits. PLL phase-locked loop technology is also adopted, effectively avoiding the jitter of the global high-frequency clock, thereby achieving synchronisation consistency with the clock.

Using a unified time base standard to extract register information from each channel: In navigation signal measurement (including pseudorange measurement, carrier Doppler measurement, etc.), a unified time base module is used to generate a global sampling clock flag to ensure that the state registers of all channels (including pseudocode period counter, pseudocode phase counter, pseudocode NCO phase word, carrier NCO phase word, and carrier period counter) are sampled at the same

time, so as to ensure the accuracy of pseudorange measurement. The register data sampled at the same time can be stored in the cache and read out by the microprocessor of the information processing module at different times. At this point, although the microprocessor operates in a time-sharing manner, the data obtained is collected at the same time and does not introduce time delay inconsistency.

i *Estimate of CV error*

In summary, the statistical value of CV errors in dynamic environments is as follows:

$$\sigma_{dev} = \sqrt{\sigma_{eph}^2 + \sigma_{rec}^2 + \sigma_{ion}^2 + \sigma_{tro}^2 + \sigma_{multipath}^2 + \sigma_{syn}^2 + \sigma_{dyn}^2} = 5.013ns \leq 10ns$$

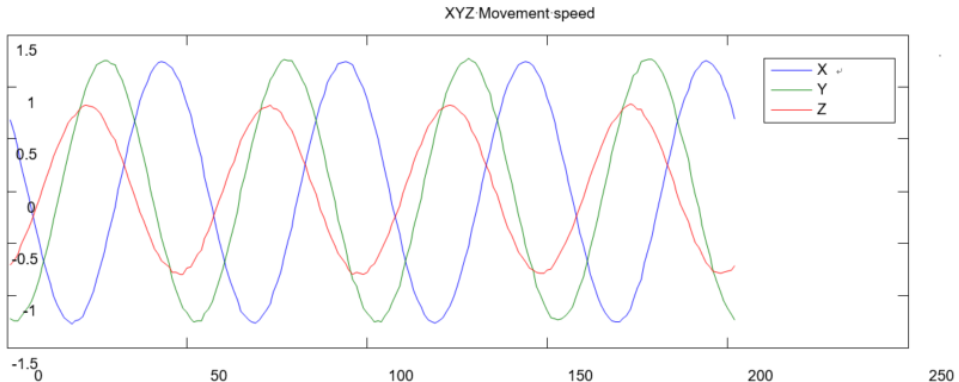
5 The test results of actual environment and simulation

5.1 Simulator testing in dynamic scene

Position accuracy and timing accuracy of the receiver are tested by simulator. In detail, situation is simulated that receiver is on the stationary ship, which is on the sea surface but is affected by wind. And they waves during ship oscillation.

The editing time of dynamic trajectory is about 1 hour. X-axis velocity is ranging from -1.3m/s to 1.3m/s (maximum displacement of 32.5m) in sinusoidal motion, Y-axis velocity is ranging from -1.3 m/s to 1.3 m/s (maximum displacement of 32.5m) in sinusoidal motion, and Z-axis velocity is ranging from -0.8m/s to 0.8m/s (maximum displacement of 20m) in sinusoidal motion. The three-axis motion velocity is shown in Figure 2.

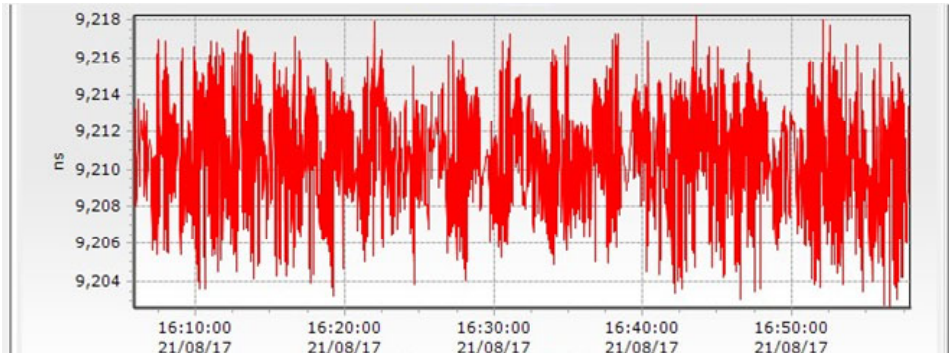
Figure 2 Dynamic environmental parameters (see online version for colours)



The dynamic scene is simulated by using a simulator, in detail, the receiver signal input interface is connected to the simulator signal output interface. And the receiver PPS and simulator PPS are connected simultaneously to the CH1 and CH2 of the second pulse comparison analyser. Then the simulator is runned, and the serial port data and PPS data are recorded after receiving the satellite and positioning normally.

The timing results of the receiver during the entire positioning process are compared with those of the simulator as shown in Figure 3.

Figure 3 Result of testing (see online version for colours)

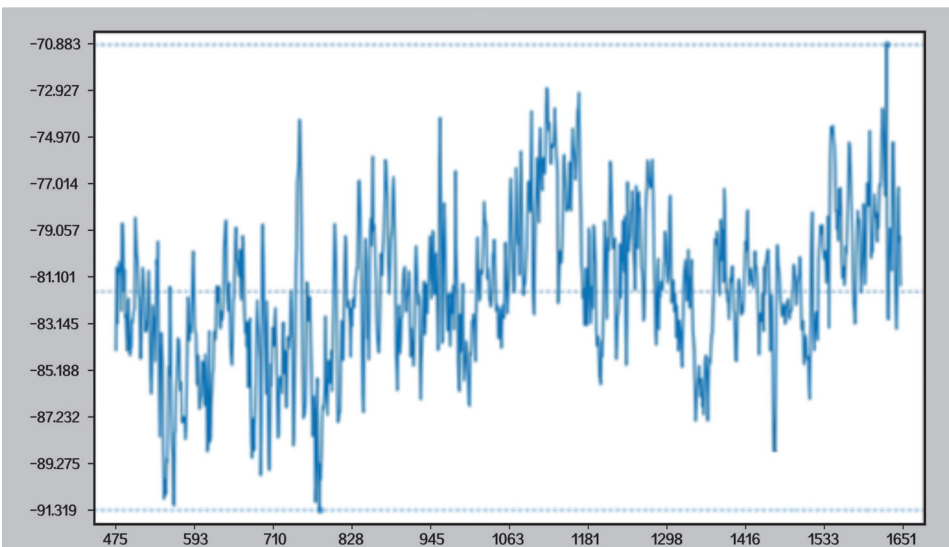


In this situation, standard deviation is 2.87ns.

5.1.1 Testing situation of rooftop mobile antenna

After using the method of position's smooth filtering with velocity in the dynamic environment, situation is simulated that the antenna was manually moved horizontally. In this situation, a short baseline CV test was conducted. It was found that there was no significant time difference jump during the movement process, with a standard deviation of 3ns. The test result is shown in Figure 4.

Figure 4 The result of testing (see online version for colours)



5.1.2 Testing situation on the lake surface

A lake surface simulation experiment was conducted at the Tiantai Mountain Reservoir in Chengdu, and a short baseline CV test was conducted (two antennas were installed on two ships, and the equipment was placed on one ship, where the CV results is evaluated by using a counter). It was found that there was no significant time difference jump during the ship's movement process, with a standard deviation of 2.19ns. The test result is shown in Figure 4.

Figure 5 Test results of lake surface environment (see online version for colours)

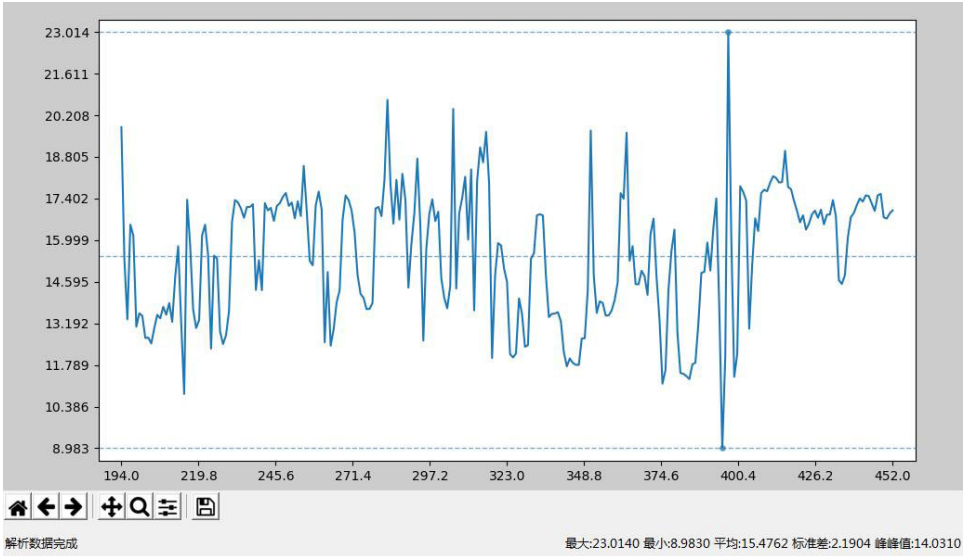


Figure 6 Lake surface testing environment (see online version for colours)



6 Conclusions

With the increasing application of cluster or formation collaborative work, the fundamental premise of unified spatiotemporal benchmarks has become increasingly important. To achieve interconnection and interoperability between computer data communication networks of platforms and various systems, precise time synchronisation is required for each platform. Only precise timing can complete the fusion processing of control instructions, target detection and other data, and maximise the efficiency of collaborative work.

This paper improves the position accuracy of the measurement station using the method of position's smooth filtering with velocity. And the position accuracy is improved to about 1m in a dynamic sea environment. After applying proposed method to CV receivers on a moving platform, it is verified through simulating sources and tested in actual environments. The results show that the CV comparison accuracy can reach 10ns under dynamic sea environment, whose synchronisation accuracy can meet the accuracy requirements of sea surface mobile platforms.

At the same time, in response to harsh and dynamic marine environments, equipment is designed with anti mould, salt spray, and other three protection measures to improve the reliability and lifespan of the equipment in marine environments. In order to ensure that the device has the ability to maintain precise time synchronisation under signal interruption conditions, a rubidium atomic clock can be configured inside the device. When the output frequency of the rubidium atomic clock is calibrated to $1E-12$, the synchronisation accuracy between devices within 1 hour can be guaranteed to be within 10ns (the drift rate of the rubidium atomic clock is $3E-12$ /day).

Acknowledgements

This work was supported by the Open Fund Project of Laboratory of Science and Technology on Marine Navigation and Control, China State Shipbuilding Corporation, Project's number: 2022010104.

References

- Andreas, B., Dirk, P., Thomas, P. et al. (2019) 'Amelioration of the usage and monitoring of GNSS signals at PTB', *Proceedings of the 50th Annual Precise Time and Time Interval Systems and Applications Meeting*, Reston, USA, 28–31 January.
- Geng, J., Chen, X., Pan, Y. et al. (2019) 'A modified phase clock/bias model to improve PPP ambiguity resolution at Wuhan University', *Journal of Geodesy*, Vol. 93, No. 10, pp.2053–2067.
- Guang, W., Zhang, J.H., Yuan, H.B. et al. (2020) 'Analysis on the time transfer performance of BDS-3 signals', *Metrologia*, Vol. 57, No. 6, p.065023, 17pp.
- Jiang, Z., Zhang, V., Parker, T.E. et al. (2019) 'Improving two-way satellite time and frequency transfer with redundant links for UTC generation', *Metrologia*, Vol. 56, No. 2, p.025005.
- Lu, X.C., Chen, L., Shen, N. et al. (2020) 'Decoding PPP corrections from BDS B2b signals using a software-defined receiver: an initial performance evaluation', *IEEE Sensors Journal*, Vol. 21, No. 6, pp.7871–7883.

- Panfilo, G., Petit, G and Harmegnies, A. (2020) 'A first step towards the introduction of redundant time links for the generation of UTC: the calculation of the uncertainties of [UTC-UTC(k)]', *Metrologia*, Vol. 57, No. 6, p.065011.
- Tavella, P. and Petit, G. (2020) 'Precise time scales and navigation systems: mutual benefits of timekeeping and positioning', *Satellite Navigation*, Vol. 1, No. 1, p.10.
- Yang, H., Yang, X. et al. (2018) 'High-precision ionosphere monitoring using continuous measurements from BDS GEO satellites', *Sensors*, Vol. 18, p.714, DOI: 10.3390/s18030714.
- Yang, Y.X., Liu, L., Li, J.L. et al. (2021) 'Featured services and performance of BDS-3', *Science Bulletin*, Vol. 66, No. 20, pp.2135–2143.
- Zhang, P.F., Tu, R., Gao, Y.P. et al. (2018) 'Improving the performance of multi-GNSS time and frequency transfer using robust Helmert variance component estimation', *Sensors*, Vol. 18, No. 9, p.2878.
- Zhou, F., Dong, D., Li, P. et al. (2019) 'Influence of stochastic modeling for inter-system biases on multi-GNSS undifferenced and uncombined precise point positioning', *GPS Solutions*, Vol. 23, No. 3, p.59.